

Nuclear magnetic moments of francium 207–213 from precision hyperfine comparisons

B. M. Roberts* and J. S. M. Ginges†

School of Mathematics and Physics, The University of Queensland, Brisbane, QLD 4072, Australia
(Dated: April 30, 2022)

We report a fourfold improvement in the determination of nuclear magnetic moments for neutron-deficient isotopes of francium-207–213, reducing the uncertainties from 2% for most isotopes to 0.5%. These are found by comparing our high-precision calculations of hyperfine structure constants for the ground states with experimental values. In particular, we show the importance of a careful modeling of the Bohr-Weisskopf effect, which arises due to the finite nuclear magnetization distribution. This effect is particularly large in Fr and until now has not been modeled with sufficiently high accuracy. An improved understanding of the nuclear magnetic moments and Bohr-Weisskopf effect are crucial for benchmarking the atomic theory required in precision tests of the standard model, in particular atomic parity violation studies, that are underway in francium.

Precision investigations of the magnetic hyperfine structure of heavy atoms play an important role in tests of the standard model at low-energy, nuclear physics models, and quantum electrodynamics [1]. The magnetic hyperfine structure refers to small splittings in the atomic spectra arising due to the interaction of the nuclear magnetic moment with atomic electrons. Comparison of calculated and observed hyperfine structure provides the best information about the accuracy of modeled atomic wavefunctions at small radial distances. This is particularly important for studies of atomic parity violation, which provide powerful tests of physics beyond the standard model [2, 3]. Experiments have been proposed [4–6] and are underway at TRIUMF [7, 8] to measure parity violation in Fr. In this atom, due to the higher nuclear charge, the tiny parity-violating effects are enhanced [9] compared to those in Cs, for which the most precise measurement has been performed [10] and a new measurement is in progress [11].

We perform high-precision calculations of the magnetic hyperfine constants \mathcal{A} for the lowest $s_{1/2}$ and $p_{1/2}$ states of $^{207-213}\text{Fr}$. We examine in detail the effect of the nuclear magnetization distribution, the Bohr-Weisskopf effect [12]. This is particularly large for the considered Fr isotopes, with relative corrections of 1.3–1.8% for s -states being 6–8 times that of ^{133}Cs , and must be treated appropriately for precision calculations. While it is standard to model this effect in heavy atoms assuming a spherical nucleus of uniform magnetization, we show this overestimates the correction by about a factor of two. Here, we employ a single-particle nuclear model (e.g., [13–15]), and demonstrate this significantly improves agreement with experiment [16, 17] for hyperfine anomalies [18]. The difference between the two models amounts to a correction to \mathcal{A} that is much larger than the atomic theory uncertainty; e.g., it is 1.4% for ^{211}Fr s -states.

Combining our calculations with experimental hyperfine constants, we extract improved values of the nuclear magnetic moments μ for $^{207-213}\text{Fr}$. The resulting uncertainty is dominated by that of the \mathcal{A} calculations. Based

on an examination of individual contributions to \mathcal{A} for Rb, Cs, and Fr, we conclude that our calculations, and thus the extracted nuclear moments, are accurate to at least 0.5%, which is up to a fourfold improvement in precision over previous values.

Hyperfine structure calculations— The relativistic operator for the magnetic hyperfine interaction is (we use atomic units $\hbar = |e| = m_e = 1$, $c = 1/\alpha$):

$$h_{\text{hfs}} = \alpha \boldsymbol{\mu} \cdot (\mathbf{r} \times \boldsymbol{\alpha}) F(r)/r^3, \quad (1)$$

where $\boldsymbol{\alpha}$ is a Dirac matrix and $\boldsymbol{\mu} = \mu \mathbf{I}/I$ with \mathbf{I} the nuclear spin. $F(r)$ describes the nuclear magnetization distribution, which will be discussed in the following sections. Matrix elements of the operator (1) can be expressed as $\mathcal{A}\langle \mathbf{I} \cdot \mathbf{J} \rangle$, where \mathbf{J} is the electron angular momentum, and \mathcal{A} is calculated using atomic wavefunctions.

For single-valence alkali atoms we employ the correlation potential method [19–21]. This method has been used, e.g., for high-precision calculations of parity violation in Cs [22–24], and was used recently by us to investigate correlation trends in \mathcal{A} for excited states [25]. The orbital φ and energy ε for the valence electron are found by solving the single-particle equation:

$$(h_{\text{HF}} + \Sigma) \varphi = \varepsilon \varphi, \quad (2)$$

where $h_{\text{HF}} = c\boldsymbol{\alpha} \cdot \mathbf{p} + (\beta - 1)c^2 + V_{\text{nuc}} + V_{\text{HF}}$, β is a Dirac matrix, and V_{nuc} and V_{HF} are the nuclear and Hartree-Fock (HF) potentials, respectively. To form V_{HF} , the set of HF equations [Eq. (2) without Σ] are solved self-consistently for the $(Z - 1)$ core electrons. To form V_{nuc} , we assume a Fermi-type nuclear charge distribution,

$$\rho(r) = \rho_0 (1 + \exp[(r - c)/a])^{-1}, \quad (3)$$

where ρ_0 is a normalization factor, c is the half-density radius, and a is defined via the 90–10% density fall-off $t \equiv 4a \ln 3 = 2.3$ fm.

In Eq. (2), Σ is the energy-dependent non-local correlation potential, through which the dominating core-valence correlations are included. This may be calculated to second (lowest) order of perturbation theory [19]

($\Sigma^{(2)}$), or to all orders [21] ($\Sigma^{(\infty)}$). We account for magnetic and retardation effects by including the Breit interaction self-consistently into the HF equations (see [26]).

To estimate the contribution of missed correlation effects, we introduce scaling factors, $\Sigma \rightarrow \lambda\Sigma$ in Eq. (2), which are tuned to reproduce experimental energies. The accuracy is already very high, so $\lambda \approx 1$ (for Fr, $\lambda_s \simeq 0.994$). To avoid double-counting, all effects must be included before the scaling is performed, including the radiative quantum electrodynamics (QED) effects. We account for these by adding the potential V_{rad} [27] into Eq. (2). The QED effects are included via V_{rad} only for the scaling of Σ . A different approach is required to include QED effects into the \mathcal{A} calculations; we take these corrections from Ref. [28] (see also [29]).

Including the hyperfine interaction, the single-particle orbitals are perturbed as $\phi + \delta\phi$ (and $\varepsilon \rightarrow \varepsilon + \delta\varepsilon$), where ϕ is the unperturbed orbital and $\delta\phi$ is the correction due to the hyperfine interaction. This leads to a perturbation, δV_{hfs} , to the HF core potential known as core polarization. To account for this, the set of equations,

$$(h_{\text{HF}} - \varepsilon_c)\delta\phi_c = -(h_{\text{hfs}} + \delta V_{\text{hfs}} - \delta\varepsilon_c)\phi_c, \quad (4)$$

is solved self-consistently for all core orbitals. Then, the hyperfine matrix elements for an atom in state v are calculated as $\langle \varphi_v | h_{\text{hfs}} + \delta V_{\text{hfs}} | \varphi_v \rangle$, which includes core polarization to all orders [19, 30]. We also include small ($\lesssim 1\%$) corrections due to non-linear combinations of the correlation and hyperfine interactions, the so-called structure radiation (SR) and normalization of states (NS) [19].

Nuclear magnetization distribution— In Eq. (1), $F(r)$ describes the nuclear magnetization distribution, and gives an important contribution to the hyperfine structure known as the Bohr-Weisskopf (BW) effect [12]. For heavy atoms, it is standard to model the nucleus as a ball of uniform magnetization, so that

$$F_{\text{Ball}}(r) = (r/r_N)^3 \quad \text{for } r < r_N, \quad (5)$$

and $F_{\text{Ball}} = 1$ for $r \geq r_N$, where $r_N = \sqrt{5/3}r_{\text{rms}}$.

Here, we use a more accurate nuclear single-particle model, that has been used in studies of QED effects in one- and few-electron ions [13–15, 31]. For the odd isotopes, we take the distribution as presented in Ref. [15]:

$$F_I(r) = F_{\text{Ball}}(r)[1 - \delta F_I \ln(r/r_N) \Theta(r_N - r)], \quad (6)$$

which includes the leading nuclear effects, though neglects corrections such as the spin-orbit interaction (see Ref. [32]). Here, Θ is the Heaviside step function, and

$$\delta F_I = \begin{cases} \frac{3(2I-1)}{8(I+1)} \frac{4(I+1)g_L - g_S}{g_I I} & I = L + 1/2 \\ \frac{3(2I+3)}{8(I+1)} \frac{4I g_L + g_S}{g_I I} & I = L - 1/2, \end{cases} \quad (7)$$

with I , L , and S respectively being the total, orbital, and spin angular momentum for the unpaired nucleon [15],

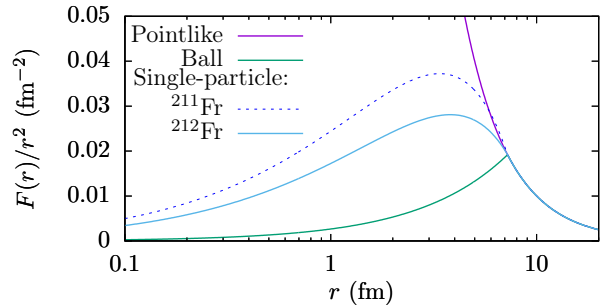


FIG. 1. Radial dependence of the hyperfine operator (1), with magnetization distribution as modeled for Fr by: a pointlike nucleus, a ball of constant magnetization, and using the single-particle nuclear model. The difference between ^{211}Fr and ^{212}Fr is due to the unpaired neutron in ^{212}Fr .

$g_L = 1(0)$ for a proton(neutron), and $g_I = \mu/(\mu_N I)$ is the nuclear g -factor with μ_N the nuclear magneton. The effective spin g -factor, g_S , is determined from the experimental g_I value using the formula:

$$g_I = \frac{1}{2} \left[g_L + g_S + (g_L - g_S) \frac{L(L+1) - S(S+1)}{I(I+1)} \right]. \quad (8)$$

For doubly-odd nuclei with both an unpaired proton and neutron, the $F(r)$ distribution can be expressed via

$$g_I F_I(r) = \beta g_I^\pi F_{I^\pi}^\pi(r) + (1 - \beta) g_I^\nu F_{I^\nu}^\nu(r), \quad (9)$$

where $F_I^{\pi/\nu}$ is the unpaired proton/neutron function (6),

$$\beta = \frac{1}{2} \left(1 + \frac{I^\pi(I^\pi + 1) - I^\nu(I^\nu + 1)}{I(I+1)} \right), \quad (10)$$

and the total nuclear spin is the sum of that of the unpaired proton and neutron: $\mathbf{I} = \mathbf{I}^\pi + \mathbf{I}^\nu$.

For the Fr isotope chain between $A = 207 - 213$, the proton configuration remains unchanged [33], and the proton g -factor for an even nucleus can be taken as that of a neighboring odd nucleus [14]. For the unpaired neutron, we determine g_I^ν from the experimental g_I and the assumed g_I^π and g_S^π using Eq. (8) with $L, S \rightarrow I^{\pi,\nu}$. The resulting distributions are shown for $^{211,212}\text{Fr}$ in Fig. 1. The data required to form F_I are presented in Table I.

The relative BW correction, ϵ , is defined via:

$$\mathcal{A}_{[F_I]} = \mathcal{A}_{[1]}(1 + \epsilon), \quad (11)$$

where $\mathcal{A}_{[F_I]}$ is calculated using the single-particle model, $F(r) = F_I(r)$, while $\mathcal{A}_{[1]}$ is calculated assuming a pointlike magnetization distribution, $F(r) = 1$; both include the finite charge distribution. Our calculations of ϵ are presented in Table I. The ϵ values are quite stable, and depend only very weakly on correlation effects [34, 35].

To test the accuracy of the nuclear models, we express Eq. (11) as $\mathcal{A} = g_I a^0(1+\delta)(1+\epsilon)$ [18], where δ is the correction due to the nuclear charge distribution. Then, a^0 is

TABLE I. Literature values for the root-mean-square charge radii (r_{rms}), magnetic moments (μ), spin (I) and parity (Π) designations, and configurations for the unpaired proton (π) and neutron (ν) for Fr nuclei. The final columns show the relative BW corrections (ϵ) determined in this work.

A	r_{rms} [36] (fm)	μ [33] (μ_N)	Config. [33]			ϵ (%)	
			I^Π	π	ν	7s	$7p_{1/2}$
207	5.5720(18)	3.89(8)	9/2 ⁻	$h_{9/2}$		-1.26	-0.37
208	5.5729(18)	4.75(10)	7 ⁺	$h_{9/2}$	$f_{5/2}$	-1.66	-0.50
209	5.5799(18)	3.95(8)	9/2 ⁻	$h_{9/2}$		-1.29	-0.38
210	5.5818(18)	4.40(9)	6 ⁺	$h_{9/2}$	$f_{5/2}$	-1.67	-0.50
211	5.5882(18)	4.00(8)	9/2 ⁻	$h_{9/2}$		-1.32	-0.39
212	5.5915(18)	4.62(9)	5 ⁺	$h_{9/2}$	$p_{1/2}$	-1.77	-0.53
213	5.5977(18)	4.02(8)	9/2 ⁻	$h_{9/2}$		-1.33	-0.40

the hyperfine constant assuming a pointlike nucleus (for both the magnetization and charge distributions) with gI factored out. Importantly, a^0 is the same for all isotopes of a given atom [37]. (The QED effect, essentially the same for each isotope, is absorbed here into a^0 .)

We form ratios using the 7s and $7p_{1/2}$ states for each of the considered Fr isotopes [16] (see also [18, 38, 39]):

$$\mathcal{R}_{sp} \equiv \frac{\mathcal{A}_s}{\mathcal{A}_p} \approx \frac{a_s^0}{a_p^0} (1 + \epsilon_s - \epsilon_p + \delta_s - \delta_p). \quad (12)$$

The term in the parenthesis (less 1) is the sp hyperfine anomaly [18]. \mathcal{R}_{sp} is independent of the nuclear moments, which for most Fr isotopes are only known to 2% [40]. A comparison between our calculations and the experimental ratios is presented in Fig. 2. The isotope dependence of \mathcal{R}_{sp} is dominated by ϵ_s (for Fr, $\epsilon_s > 3\epsilon_p$).

Though $|\delta| > |\epsilon|$, δ is modeled accurately by the charge distribution (3), and changes only slightly between nearby isotopes. We quantify possible errors in δ by making adjustments to the c and t values in Eq. (3), and find the resulting uncertainties to be negligible.

Since the proton configuration remains unchanged, the differences in \mathcal{R} along the isotope chain are due to the contribution of the unpaired neutron to the BW effect, $\epsilon^{(\nu)}$ (see Fig. 2). Thus, we can cleanly extract $\epsilon^{(\nu)}$ from the ratio of \mathcal{R} between neighboring isotopes. Comparing our values to experimental ratios [16, 17], we find that we reproduce $\epsilon^{(\nu)}$ to between 5 and 35%. The neutron contributes about 30% to the total ϵ , see Table I.

To gauge the accuracy of the calculated proton contribution to ϵ , we examine \mathcal{R} for the odd isotopes. While \mathcal{R} does not depend on the nuclear moments, it does depend on the electron wavefunctions, and the difference between the theory and experiment is likely dominated by errors in the electron correlations. We therefore re-scale \mathcal{R} for Fr by the factor $\xi = \mathcal{R}_{sp}^{\text{Expt.}}(^{133}\text{Cs})/\mathcal{R}_{sp}^{\text{Th.}}(^{133}\text{Cs})$, which corrects the Cs \mathcal{R} value, and amounts to a shift of smaller than 1%. The relative correlation corrections between Cs and Fr are similar [25], so this is expected to roughly ac-

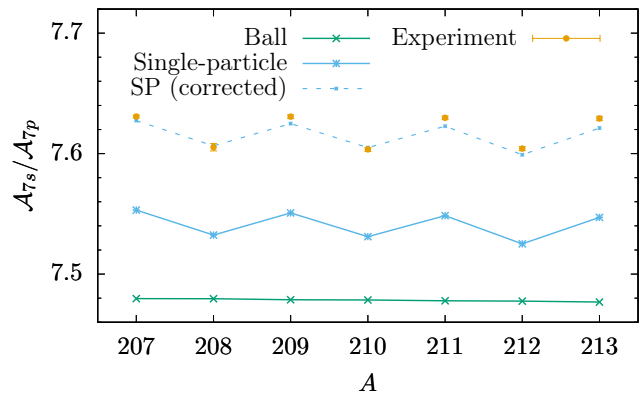


FIG. 2. Calculated ratios of the 7s to $7p_{1/2}$ hyperfine constants for $^{207-213}\text{Fr}$ using the ball and single-particle (SP) nuclear magnetization models, and comparison with experiment [17]. The odd-even staggering is due to the addition of neutrons; the slight negative slope is due to the changing nuclear radius. The dashed blue line shows the calculated (SP) ratios corrected by the factor $\xi(^{133}\text{Cs})$; see text for details.

count for correlation errors in $\mathcal{R}(\text{Fr})$. After re-scaling, we find agreement with experiment to 0.1% (dashed line in Fig. 2). Since the relative s -state BW effect is an order of magnitude larger for Fr than for Cs [41], this provides a good method for testing the accuracy of the Fr BW correction. The BW effect contributes about 1% to \mathcal{R} , implying we accurately reproduce the proton contribution to the BW effect to about 10%. A similar result is reached if we instead re-scale by the Rb ξ factor. We therefore conclude that the BW effect is calculated accurately, and take the uncertainty to be 20%.

Results and discussion— In Table II, we present our calculated hyperfine constants for ^{87}Rb , ^{133}Cs , and ^{211}Fr , along with experimental values for comparison. Note that for Fr the uncertainty in the calculated \mathcal{A} is dominated by that of the literature value for μ . The ratio $\mathcal{A}^{\text{Th.}}/\mu$, however, is independent of this uncertainty.

To estimate the theoretical uncertainty, we assigned errors individually for each of the important contributions, which are presented separately in Table II. These are taken as twice the difference between the fitted and unfitted correlation potentials ($\lambda\Sigma$ row), and 20% for each of the combined structure radiation and normalization of states (SR+NS), Breit, and BW contributions. We take QED uncertainties of 15–20% from Ref. [28]. This leads to theoretical uncertainties of approximately 0.6%, 0.5%, and 0.5%, for Rb, Cs, and Fr, respectively. We believe these are conservative estimates, justified by the very good agreement between theory and experiment for Rb and Cs (0.4% and 0.2%, respectively). Further, recent calculations using the same method for the $^{135}\text{Ba}^+$ and $^{225}\text{Ra}^+$ ions also have excellent agreement with experiment, both with discrepancies of about 0.2% [28].

TABLE II. Contributions to the ground-state hyperfine constants \mathcal{A} (in MHz) for ^{87}Rb , ^{133}Cs , and ^{211}Fr . The last two rows show the discrepancy between theory and experiment. The Fr calculations assumed $\mu = 4.0\mu_N$, which has a 2% uncertainty [33]; the resulting 2% uncertainties for the Fr calculations are shown in italics.

	^{87}Rb (5s)	^{133}Cs (6s)	^{211}Fr (7s)
HF	2183.1	1433.7	5929.2
δV_{hfs}	460.3	294.4	1111.2
$\Sigma^{(2)}$	980.7	779.6	2622.6
$\Sigma^{(\infty)} - \Sigma^{(2)}$	-171.1	-170.0	-480.6
$(\lambda - 1)\Sigma^{(\infty)}$	9.3	-5.1	-13.1
SR+NS	-48.0	-31.9	-129.0
Breit	6.0	5.9	33.0
Subtotal	3420(21)	2307(12)	9073(37)(181)
BW	-9.5(1.9)	-4.8(1.0)	-120(24)
QED [28]	-8.3(1.2)	-8.8(1.5)	-55(12)
Total	3403(21)	2293(12)	8899(46)(178)
Expt. [42]	3417.341...	2298.157...	8713.9(8)
Δ (MHz)	-14.8	-5.1	185 (178)
Δ (%)	-0.43%	-0.22%	2.1 (2.0)%

Our calculations for Fr are also in excellent agreement with those of previous calculations that use a different method [43, 44], with deviations of just 0.1–0.2%, so long as the BW effect, which has been modeled more accurately by us, and the QED corrections, which were neglected in [43, 44], are accounted for.

By combining the high-precision calculations from this work with the measured values for the hyperfine structure constants, improved values for the Fr nuclear magnetic moments can be deduced. These are extracted as

$$\mu = (\mathcal{A}_{7s}^{\text{Expt.}} / \mathcal{A}_{7s}^{\text{Th.}}) \tilde{\mu}, \quad (13)$$

where $\tilde{\mu}$ are the values used as inputs in the calculations (μ in Table I). Since the experimental \mathcal{A} values are known to $\lesssim 0.01\%$, the uncertainty is dominated by that of the theory. The final calculated hyperfine constants for $^{207-213}\text{Fr}$ and the resulting recommended values for the nuclear moments are presented in Table III.

Most of the considered experimental values for μ come from a single experiment [33]. In that work, the values for $^{207-213}\text{Fr}$ were deduced from measurements made on ^{211}Fr , so the experimental uncertainties are not independent. Our extracted values agree with those values within the uncertainties, though are all about 2% smaller.

A more recent result is available for ^{210}Fr , which comes from a combination of a measurement and calculation of \mathcal{A} for the excited 9s state [43]. The theory portion of that work used a ball model for the magnetization distribution, and did not include QED effects. If we re-scale the calculations from Ref. [43] to correct for the BW and QED effects as described above, their value for the ^{210}Fr magnetic moment changes from $\mu = 4.38\mu_N$ to $4.36\mu_N$ using \mathcal{A}_{9s} , or to $4.33\mu_N$ using \mathcal{A}_{7s} , which are both in

TABLE III. Final theory values for the ground-state hyperfine constant \mathcal{A}_{7s} for $^{207-213}\text{Fr}$, assuming the literature μ values and theoretical BW corrections presented in Table I, alongside other values for comparison. Note the μ values from Ref. [33] were deduced from measurements made on ^{211}Fr . The final column shows the recommended values for the magnetic moments as determined in this work.

A	\mathcal{A}_{7s}		μ/μ_N	
	Expt.	Theory	Others	This work
207	8484(1) [45]	8664(45)	3.89(8) [33]	3.81(2)
208	6650.7(8) [45]	6773(35)	4.75(10) [33]	4.67(3)
	6653.7(4) [46]		4.71(4) ^a [46]	
209	8606.7(9) [45]	8793(46)	3.95(8) [33]	3.87(2)
210	7195.1(4) [45]	7317(38)	4.40(9) [33]	4.33(3)
			4.38(5) ^a [43]	
211	8713.9(8) [45]	8899(46)	4.00(8) [33]	3.92(2)
212	9064.2(2) [45]	9209(48)	4.62(9) [33]	4.55(3)
213	8759.9(6) [45]	8943(47)	4.02(8) [33]	3.94(2)

^a These values for ^{208}Fr [46] and ^{210}Fr [43] change to 4.66(4) and 4.33(5), respectively, when corrected to account for the QED and BW effects; see text for details.

agreement with our value. We note that our calculations [25], as well as those from Refs. [43, 44], reproduce the Rb and Cs experimental \mathcal{A} values for the ground states with higher accuracy than for the excited states (see Ref. [25]). Therefore, we feel it is more accurate to extract μ using the Fr 7s ground state.

A more recent measurement of $\mu(^{208}\text{Fr})$ is also available [46]. However, this value and those for $^{204-206}\text{Fr}$ were found in [46] using the $\mu(^{210}\text{Fr})$ result of Ref. [43] as a reference. As explained above, these should be corrected to account for the QED and BW effects. The corrected result for $\mu(^{208}\text{Fr})$ is $4.66(4)\mu_N$, coinciding with our result $4.67(3)\mu_N$.

Conclusion— By combining high-precision calculations with measured values for the ground-state magnetic hyperfine constants, we have extracted new values for the nuclear magnetic moments of $^{207-213}\text{Fr}$. In particular, we show the importance of an accurate modeling of the nuclear magnetization distribution, the so-called Bohr-Weisskopf effect, which until now has not been modeled with sufficiently high accuracy for Fr. We model this effect using a simple nuclear single-particle model, which gives greatly improved agreement for hyperfine anomalies. We conclude that the single-particle model should be used rather than the ball model in future high-precision calculations. Our extracted nuclear magnetic moments are about 2% smaller than existing literature values, which mostly come from a single experiment. Based on our analysis, we expect our results to be accurate to 0.5%, a factor of four improvement in precision over previous values for most isotopes.

Acknowledgments— This work was supported by the Australian Government through an Australian Research Council Future Fellowship, Project No. FT170100452.

-
- * b.roberts@uq.edu.au
† j.ginges@uq.edu.au
- [1] M. S. Safronova, D. Budker, D. DeMille, D. F. J. Kimball, A. Derevianko, and C. W. Clark, *Rev. Mod. Phys.* **90**, 025008 (2018).
- [2] J. S. M. Ginges and V. V. Flambaum, *Phys. Rep.* **397**, 63 (2004).
- [3] B. M. Roberts, V. A. Dzuba, and V. V. Flambaum, *Annu. Rev. Nucl. Part. Sci.* **65**, 63 (2015), [arXiv:1412.6644](https://arxiv.org/abs/1412.6644).
- [4] J. A. Behr, S. B. Cahn, S. B. Dutta, A. Gorlitz, A. Ghosh, G. Gwinner, L. A. Orozco, G. D. Sprouse, and F. Xu, *Hyperfine Interact.* **81**, 197 (1993).
- [5] V. A. Dzuba, V. V. Flambaum, and O. P. Sushkov, *Phys. Rev. A* **51**, 3454 (1995).
- [6] V. A. Dzuba, V. V. Flambaum, and J. S. M. Ginges, *Phys. Rev. A* **63**, 062101 (2001).
- [7] S. Aubin, J. A. Behr, R. Collister, V. V. Flambaum, E. Gomez, G. Gwinner, K. P. Jackson, D. Melconian, L. A. Orozco, M. R. Pearson, D. Sheng, G. D. Sprouse, M. Tandecki, J. Zhang, and Y. Zhao, *Hyperfine Interact.* **214**, 163 (2013).
- [8] M. Tandecki, J. Zhang, R. Collister, S. Aubin, J. A. Behr, E. Gomez, G. Gwinner, L. A. Orozco, and M. R. Pearson, *J. Instrum.* **8**, P12006 (2013).
- [9] M.-A. Bouchiat and C. C. Bouchiat, *J. Phys. France* **35**, 899 (1974); *J. Phys. France* **36**, 493 (1975).
- [10] C. S. Wood, S. C. Bennett, D. Cho, B. P. Masterson, J. L. Roberts, C. E. Tanner, and C. E. Wieman, *Science* **275**, 1759 (1997).
- [11] G. Toh, A. Damitz, C. E. Tanner, W. R. Johnson, and D. S. Elliott, *Phys. Rev. Lett.* **123**, 073002 (2019), [arXiv:1905.02768](https://arxiv.org/abs/1905.02768).
- [12] A. Bohr and V. F. Weisskopf, *Phys. Rev.* **77**, 94 (1950); A. Bohr, *Phys. Rev.* **81**, 331 (1951).
- [13] V. M. Shabaev, *J. Phys. B* **27**, 5825 (1994).
- [14] V. M. Shabaev, M. B. Shabaeva, and I. I. Tupitsyn, *Phys. Rev. A* **52**, 3686 (1995).
- [15] A. V. Volotka, D. A. Glazov, I. I. Tupitsyn, N. S. Oreshkina, G. Plunien, and V. M. Shabaev, *Phys. Rev. A* **78**, 062507 (2008), [arXiv:0806.1121](https://arxiv.org/abs/0806.1121).
- [16] J. S. Grossman, L. A. Orozco, M. R. Pearson, J. E. Sim-sarian, G. D. Sprouse, and W. Z. Zhao, *Phys. Rev. Lett.* **83**, 935 (1999).
- [17] J. Zhang, M. Tandecki, R. Collister, S. Aubin, J. A. Behr, E. Gomez, G. Gwinner, L. A. Orozco, M. R. Pearson, and G. D. Sprouse, *Phys. Rev. Lett.* **115**, 042501 (2015).
- [18] J. R. Persson, *At. Data Nucl. Data Tables* **99**, 62 (2013).
- [19] V. A. Dzuba, V. V. Flambaum, P. G. Silvestrov, and O. P. Sushkov, *J. Phys. B* **20**, 1399 (1987).
- [20] V. A. Dzuba, V. V. Flambaum, P. G. Silvestrov, and O. P. Sushkov, *Phys. Lett. A* **131**, 461 (1988).
- [21] V. A. Dzuba, V. V. Flambaum, and O. P. Sushkov, *Phys. Lett. A* **140**, 493 (1989); V. A. Dzuba, V. V. Flambaum, A. Y. Kraftmakher, and O. P. Sushkov, *Phys. Lett. A* **142**, 373 (1989).
- [22] V. A. Dzuba, V. V. Flambaum, and O. P. Sushkov, *Phys. Lett. A* **141**, 147 (1989).
- [23] V. A. Dzuba, V. V. Flambaum, and J. S. M. Ginges, *Phys. Rev. D* **66**, 076013 (2002).
- [24] V. A. Dzuba, J. C. Berengut, V. V. Flambaum, and B. M. Roberts, *Phys. Rev. Lett.* **109**, 203003 (2012), [arXiv:1207.5864](https://arxiv.org/abs/1207.5864).
- [25] S. J. Grunefeld, B. M. Roberts, and J. S. M. Ginges, *Phys. Rev. A* **100**, 042506 (2019), [arXiv:1907.02657](https://arxiv.org/abs/1907.02657).
- [26] W. R. Johnson, *Atomic Structure Theory* (Springer, New York, 2007).
- [27] V. V. Flambaum and J. S. M. Ginges, *Phys. Rev. A* **72**, 052115 (2005).
- [28] J. S. M. Ginges, A. V. Volotka, and S. Fritzsche, *Phys. Rev. A* **96**, 062502 (2017), [arXiv:1709.07725](https://arxiv.org/abs/1709.07725).
- [29] J. Sapirstein and K. T. Cheng, *Phys. Rev. A* **67**, 022512 (2003); *Phys. Rev. A* **74**, 042513 (2006).
- [30] V. A. Dzuba, V. V. Flambaum, and O. P. Sushkov, *J. Phys. B* **17**, 1953 (1984).
- [31] M. Le Bellac, *Nucl. Phys.* **40**, 645 (1963).
- [32] V. M. Shabaev, M. Tomaselli, T. Kühn, A. N. Artemyev, and V. A. Yerokhin, *Phys. Rev. A* **56**, 252 (1997).
- [33] C. Ekström, L. Robertsson, and A. Rosén, *Phys. Scr.* **34**, 624 (1986).
- [34] J. S. M. Ginges and A. V. Volotka, *Phys. Rev. A* **98**, 032504 (2018), [arXiv:1707.00551](https://arxiv.org/abs/1707.00551).
- [35] E. A. Konovalova, Y. Demidov, M. G. Kozlov, and A. Barzakh, *Atoms* **6**, 39 (2018), [arXiv:1805.10135](https://arxiv.org/abs/1805.10135).
- [36] I. Angeli and K. Marinova, *At. Data Nucl. Data Tables* **99**, 69 (2013).
- [37] We note that we don't directly calculate a^0 , this is just an instructive factorization.
- [38] S. Büttgenbach, *Hyperfine Interact.* **20**, 1 (1984).
- [39] J. R. Persson, *Eur. Phys. J. A* **2**, 3 (1998).
- [40] N. J. Stone, *At. Data Nucl. Data Tables* **90**, 75 (2005).
- [41] For Cs, we have $\epsilon_s = -0.21\%$ and $\epsilon_p = -0.01\%$, while for Fr we have $\epsilon_s = -1.3\%$, $\epsilon_p = -0.4\%$.
- [42] E. Arimondo, M. Inguscio, and P. Violino, *Rev. Mod. Phys.* **49**, 31 (1977).
- [43] E. Gomez, S. Aubin, L. A. Orozco, G. D. Sprouse, E. Iskrenova-Tchoukova, and M. S. Safronova, *Phys. Rev. Lett.* **100**, 172502 (2008).
- [44] M. S. Safronova, W. R. Johnson, and A. Derevianko, *Phys. Rev. A* **60**, 4476 (1999), [arXiv:9906044](https://arxiv.org/abs/9906044) [physics].
- [45] A. Coc, C. Thibault, F. Touchard, H. T. Duong, P. Juncar, S. Liberman, J. Pinar, J. Lermé, J. Vialle, S. Büttgenbach, A. Mueller, A. Pesnelle, and The ISOLDE Collaboration, *Phys. Lett. B* **163**, 66 (1985).
- [46] A. Voss, F. Buchinger, B. Cheal, J. E. Crawford, J. Dilling, M. Kortelainen, A. A. Kwiatkowski, A. Leary, C. D. P. Levy, F. Mooshammer, M. L. Ojeda, M. R. Pearson, T. J. Procter, and W. A. Tamimi, *Phys. Rev. C* **91**, 044307 (2015).